A library of H band stellar spectra for stellar population analysis purposes[*]

R. Dallier, C. Boisson and M. Joly

DAEC, Observatoire de Paris, Université Paris VII, CNRS (UA 173), F-92195 Meudon Cedex, France

Abstract. — A sample of 37 stars of luminosity classes I, III, V, including few SMR stars observed in the H band with a medium resolution (R=1500−2000) is presented. This sample of flux calibrated spectra is intended to widen existing stellar libraries. A new IR spectrograph, ISIS/IR, foreseen for CFHT has been used. Its main characteristics are briefly described. Stellar spectra obtained with this new spectrograph are compared to similar data obtained with the ESO NTT IRSPEC spectrograph. The behaviour of some prominent features is described and it is shown that the COλ1.60/SiIλ1.60 line ratio is a good luminosity indicator for stellar types later than K0.

Key words: line: identification — stars: fundamental parameters: classification — stars: late type — Infrared: stars — atlases

1. Introduction

A very promising wavelength range not yet fully explored to study the stellar populations of the central part of galaxies is the near IR range where cool star spectrum peaks. The H window is particularly well designed for such a study as the non-stellar contribution (mainly dust) is smaller in the H window than in the K window. For example, it has been shown by Origlia et al. (1993) that, in NGC 1068, the non-stellar contribution is only 30% in the H window while it is about 80% in the K window. Furthermore, these authors have shown that the line ratio COλ1.62/SiIλ1.59 increases strongly from early K to M stars and can be a crucial tool in the determination of the average spectral type in a stellar cluster.

As we are involved in the study of the stellar populations of active galactic nuclei, we need to compare the observed galactic spectra to stellar libraries of similar resolution. The compilation has to include the whole range of spectral types and luminosity classes.

Few stellar libraries are up to now available in the near IR. Each of them being constructed in a specific purpose, they are generally not exhaustive. Moreover some of them are restricted to the K band (Arnaud et al. 1989; Bell et al. 1990; Kleinmann & Hall 1986; see also, although less exhaustive, Casali & Mathews 1992; Gaffney & Lester 1992).

Send offprint requests to: R. Dallier

[*]Based on observations collected at the Canadian-French-Hawaiian Telescope, Hawaii, and at the European Southern Observatory, La Silla, Chile

In the H band, the more exhaustive library is by Lançon & Rocca-Volmerange (1993) with 22 dwarf, 23 giant and 10 supergiant stars but with a poor spectral resolution (R=500). Origlia et al. (1993), with a better resolution (R=1500), present a sample of 13 supergiant stars of all types, 7 cool giant and 2 dwarf stars. Other authors restrict their study to K and M stars: Terndrup et al. (1991) study 32 giant M stars with a resolution R=1000; Davidge (1990) and Davidge & Boeshaar (1993) study few K and M stars (giant and dwarf) with a low resolution (R=300 and 600). High resolution spectroscopy is also available in the near IR. Note for example the work of Mould (1978) who presents the spectra of six M dwarf stars in the H and K bands (R=2 10^4), as well as the work of Tsuji (1986, 1991) on the first or second overtone of CO in cool giant stars ($R > 5.10^4$). Unfortunately, equivalent widths or line indices of prominent features are not always given by the authors and the spectra not easily available.

Very few super metal rich stars (SMR) are included in these stellar libraries (3 in Lançon & Rocca-Volmerange 1993; and 5 in Origlia et al. 1993).

The inclusion of SMR stars in a stellar library dedicated to the study of stellar populations in the central part of galaxies is crucial as abundance gradients have been observed in the optical range with overabundances as high as a factor 5 compared to the solar vicinity (Cayrel de Strobel 1991; Vila-Costas & Edmunds 1992; Davidge 1992; Delisle & Hardy 1992).

In conclusion, we need to widen the previous data banks according to our purpose. We can use as a basis

the stellar library from Origlia et al. (1993) which has a resolution close to the one we use for our galactic spectra ($R \simeq 1500-2000$). It has to be extended with stellar spectra of different spectral types and luminosity classes including SMR stars.

We present here stellar spectra of intermediate resolution in the H band, covering a large range of spectral types and luminosity classes, and including few SMR stars. These spectra have been mainly obtained with a new IR spectrograph which is quickly introduced in the next section. In Sect. 3 we describe the observations. The libraries are presented in Sect. 4 with comments on the behaviour of some prominent features.

Table 1.

Star	Type	Tel.	Spectro.	[Fe/H]	Ref.
BS 2456	O7	CFHT	ISIS/IR	-0.09	C&92
BS 1879	O8	CFHT	ISIS/IR		
BS 1123	B0V	CFHT	ISIS/IR		
* BS 5056	B1V	CFHT	ISIS/IR		
BS 4590	B1.5V	CFHT	ISIS/IR		
* BS 4638	B3V	NTT	IRSPEC2		
BS 4456	B4V	CFHT	ISIS/IR		
BS 788	F9V	CFHT	ISIS/IR		
* BS 4983	G0V	CFHT	ISIS/IR	0.02	C&92
HD 160691	G5V	NTT	IRSPEC2	0.16	C&92
* BS 4550	G8V	CFHT	ISIS/IR	-1.40	C&92
HD 112758	K0V	CFHT	ISIS/IR		
HD 93800	K0V	NTT	IRSPEC2	0.43	BG90
		CFHT	ISIS/IR		
HD 130871	K2V	NTT	IRSPEC2		
HD 115404	K2V	CFHT	ISIS/IR		
HD 157881	K7V	NTT	IRSPEC2	0.40	C&92
GL 382	M2V	NTT	IRSPEC2		
		CFHT	ISIS/IR		
BS 1790	B2III	CFHT	ISIS/IR		
* BS 4883	G0III	CFHT	ISIS/IR	-0.27	T91
* BS 3903	G7III	CFHT	ISIS/IR	-0.14	McW90
* BS 5020	G8III	NTT	IRSPEC2	-0.12	McW90
		CFHT	ISIS/IR		
* BS 4695	K0III	NTT	IRSPEC2	-0.20	C&92
		CFHT	ISIS/IR		
BS 5315	K3III	CFHT	ISIS/IR	-0.39	McW90
* BS 5824	K3III	NTT	IRSPEC2	-0.12	McW90
BS 6973	K3III	NTT	IRSPEC2	-0.18	McW90
HD 111180	K3III	CFHT	ISIS/IR	0.25	Z91
HD 175674	K3III	NTT	IRSPEC2	0.29	C&92
BS 2731	K5III	CFHT	ISIS/IR		
HD 109655	K5III	CFHT	ISIS/IR		
BS 4174	M0III	NTT	IRSPEC2		
BS 4127	M1III	CFHT	ISIS/IR		
BS 4902	M3III	NTT	IRSPEC2		
		CFHT	ISIS/IR		
* BS 4133	B1Ib	CFHT	ISIS/IR		
BS 3459	G1I	CFHT	ISIS/IR	-0.11	C&92
BS 2764	K3I	CFHT	ISIS/IR	0.15	C&92
BS 1112	K4Ib	CFHT	ISIS/IR		
BS 5645	K4I	NTT	IRSPEC2		
BS 3170	M1Ib	CFHT	ISIS/IR		
BS 3364	M2I	CFHT	ISIS/IR		

Note to Table 1:
BG90 : Barbuy & Grenon, 1990
C&92 : Cayrel et al., 1992
McW90: McWilliam, 1990
T91 : Taylor, 1991
Z91 : Zhou, 1991

Table 2. Line identification

ident.	λ	reference name	integration bounds
HI 4-15	1.5701		
MgI	1.5750		
			1.5755
OH(3,1)P(7)	1.5760		
MgI	1.5770		
FeI	1.5778	CO 1.58	
CO(4,1)	1.5780		
FeI	1.5793		
			1.5805
FeI	1.5817		
FeI	1.5820		
SiI	1.5838	SiI+FeI	
FeI	1.5840		
			1.5854
FeI	1.5868		
FeI	1.5870	FeI	
			1.5872
HI 4-14	1.5881		
SiI	1.5892	SiI 1.59	
			1.5903
FeI	1.5909	FeI 1.591	
			1.5914
FeI	1.5916		
FeI	1.5925	FeI 1.592	
			1.5934
FeI	1.5938		
SiI	1.5964	SiI 1.60	
			1.5973
CO(5,2)	1.598	CO 1.60	
FeI	1.5985		
			1.5996
FeI	1.6013	FeI 1.60	
			1.6030
OH(3,1)P(9)	1.604	OH 1.60	
FeI	1.6046		
			1.6058
SiI	1.6064		
FeI	1.6074	SiI+FeI	
			1.6085
SiI	1.6099		
FeI	1.6107		
HI 4-13	1.6109	SiI+FeI	
FeI	1.6130		
			1.6143
CaI	1.6155		
FeI	1.6158	FeI+CaI	
			1.6171
FeI	1.6184		
CO(6,3)	1.6187	CO 1.62	
			1.6190
CaI+FeI	1.6201	CaI 1.62	
SiI+FeI	1.6220		
			1.6225
FeI	1.6236		
SiI	1.6246	FeI+OH	
OH(2,0)P(15)	1.626		
			1.6266
FeI	1.6289	FeI 1.629	
			1.6296
FeI	1.6325		
FeI	1.6329	FeI 1.63	
			1.6343
NiI	1.6368		
SiI	1.6385	NiI+SiI	
			1.6387
FeI	1.6402		
CO(7,4)	1.640	CO 1.64	
HI 4-12	1.6407		
			1.6424

2. The ISIS/IR spectrograph

ISIS/IR is a fibre-fed, 'warm' grating spectrograph, working in the J and H bands ($1.0\,\mu$m $\leq \lambda \leq 1.8\,\mu$m). It is a field spectrograph, i.e. it is possible to record spectra of contiguous points in a small field of view (up to $12''$ diameter on the sky). It is now designed to work with one of the Canada-France-Hawaii Telescope (CFHT) RedEye camera (Simons 1993). The spectrograph is mounted on
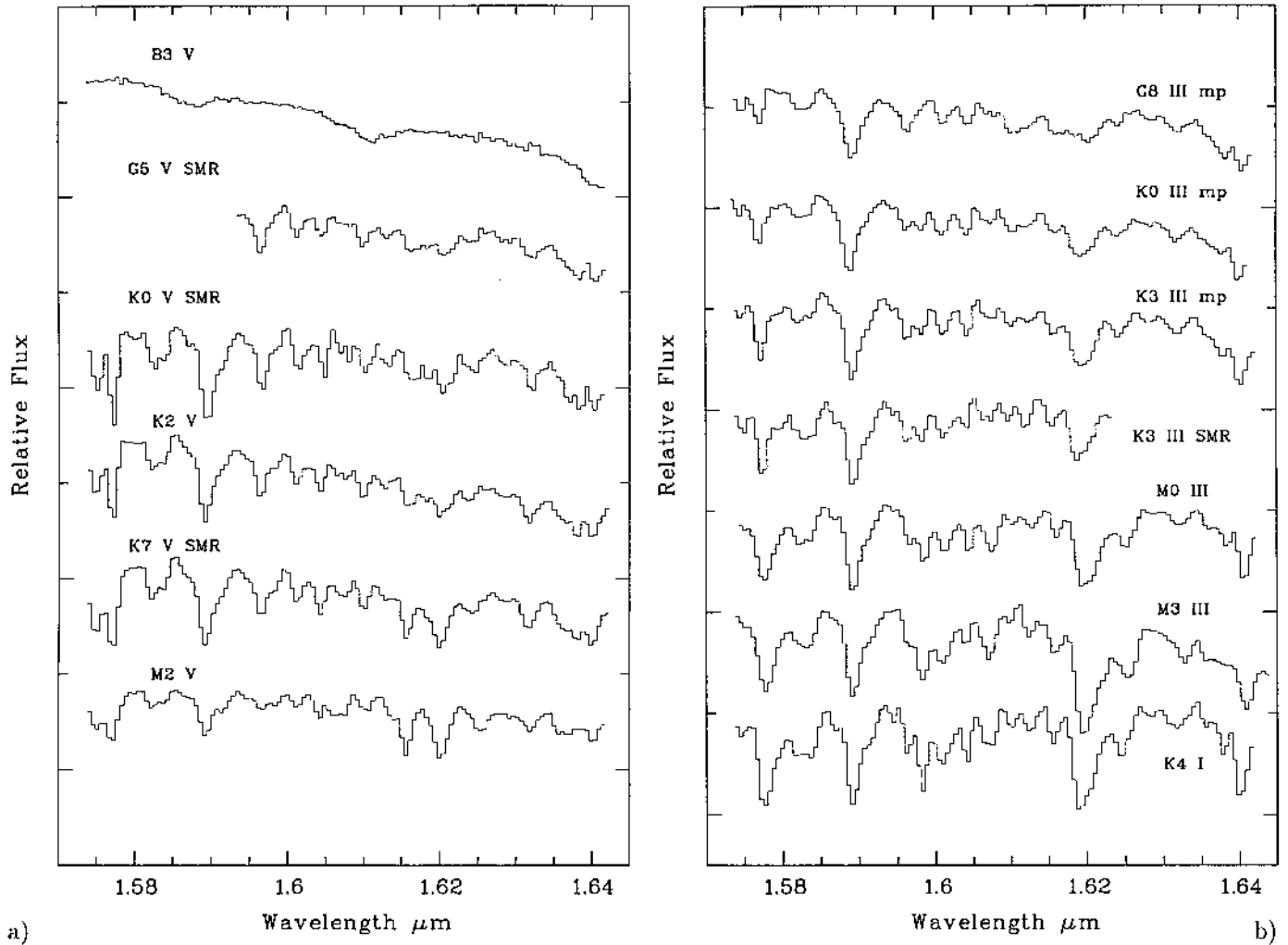
Fig. 1. a-b) The IRSPEC sample, resolution R=1500. Spectra are plotted in relative fluxes normalized to 1. in the range $1.59290-1.59506$ μm. In Fig. 1a, the shift between two spectra is 1.25, in Fig. 1b, it is 1.0

an optical bench, and coupled to the telescope with a fibre bundle. It is set on the dome floor, independent from the telescope motions. Following the light path, one can find:

- the so-called '*fibre-environment*', attached to the Cassegrain focal plane. In a general way, this device provides 3 functions: focal reduction, guiding and calibration (tungsten and argon sources for flat-field and spectral calibration). At the CFHT, the MOS-SIS bonnette serves as a fibre environment, fulfilling all the required functions.
- the *fibre bundle*. 'Dry-silica' fibres are used, providing more than 90% of internal transmission in J and H bands over a 15 meter length. 51 fibres sample the object at the focal plane, while 10 surrounding fibres simultaneously record the sky around the object. Fibre to fibre sampling is adjustable, with a focal reducer,

from 0.7 to 1.2″ per fibre. Fibres are aligned at the spectrograph side, forming a pseudo-slit that covers the 256 pixels height of the NICMOS 3 chip. This configuration allows to sample a little extended object and thus offers the possibility of spectro-imaging.
- the *spectrograph* itself. The design is based on a classical Ebert-Fastie configuration with a parabolic mirror, which provides a good image quality over the whole detector. Two resolving powers are currently available (around 400 and 2000 in both J and H).

For a resolving power of R=400 and one hour exposure (1 arcsec object, 10σ detection), the limiting magnitude is $m_J = 17$ to 18 in the J band (5 to 2 10^{-16} W/m^2/μm), and $m_H = 16$ to 17 in H (about the same flux). For $R= 2000$, $m_J = 15$ to 16 (30 to 12 10^{-16} W/m^2/μm), $m_H = 15$ (12 10^{-16} W/m^2/μm). The performances and
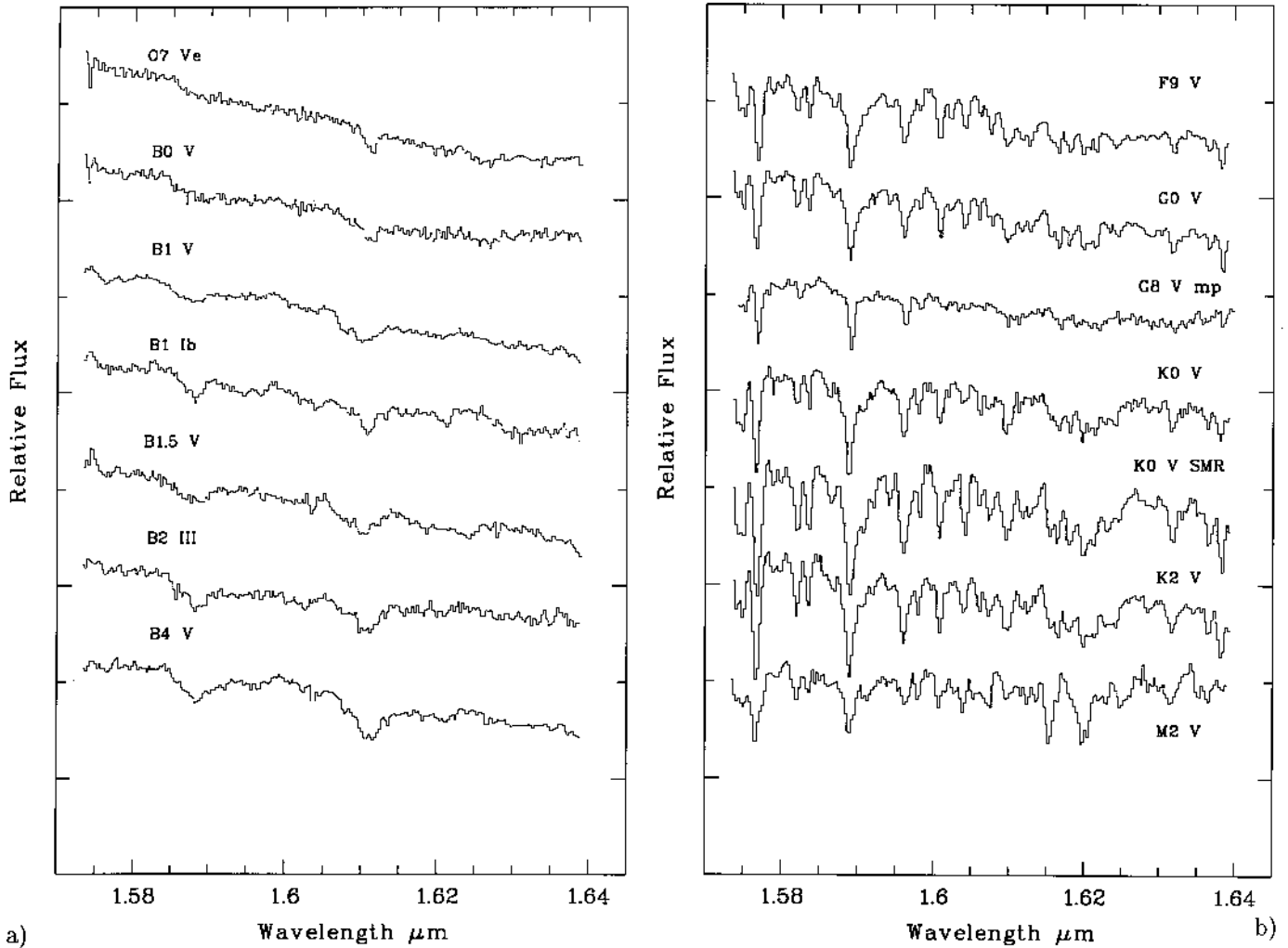
Fig. 2. a-d) The ISIS sample, resolution R=2000. Spectra are plotted in relative fluxes normalized to 1. in the range 1.59290−1.59506 μm. In Fig. 2a-c the shift between two spectra is 1.0, in Fig. 2d, it is 1.5

design of ISIS/IR are described in details in Dallier (1995).

3. Observations

During runs mainly dedicated to the observation of central parts of active galactic nuclei, two samples of stars have been observed under the same conditions as the galactic nuclei. A sample of 12 stars has been observed with IRSPEC at the ESO-NTT telescope in april 1992. The detector is a 58x62 SBRC pixel array. Grating 2 at order 1 (see Gredel & Moorwood 1991) and a 2-pixel wide slit give a spectral resolution R≃1500 at 1.60 μm. For each star we obtained spectra at 3 different grating positions, with an overlap of 30 pixels, to cover the full wavelength range of interest.

The second sample contains 30 stars observed with ISIS/IR (see Sect. 2) at the CFHT in january 1994. The focal reducer used gives a sampling of 1.2″ per fibre; each fibre projects onto about 3 NICMOS pixels. With the 300 lines/mm grating a resolution R≃2000 is achieved. The wavelength domain is covered in one ISIS observation.

In Table 1 are given a list of the stars with their spectral type and metallicity ([Fe/H]) when it is known, together with the telescope and spectrograph used. Metallicities are taken from Cayrel de Strobel et al. (1991), unless a reference is quoted in the last column.

The NTT data have been reduced using the IRSPEC context in the ESO-MIDAS package. Each frame was dark subtracted and flat-fielded using an internal halogen lamp at same wavelength and similar counts level. Observations of the stars were made with the source at two different slit positions (typical offset along the slit was of 30″) for subsequent integrations. First order sky subtraction was then easy. In case of poor cancelation of sky emission (that happens for some of the least bright stars or when weather
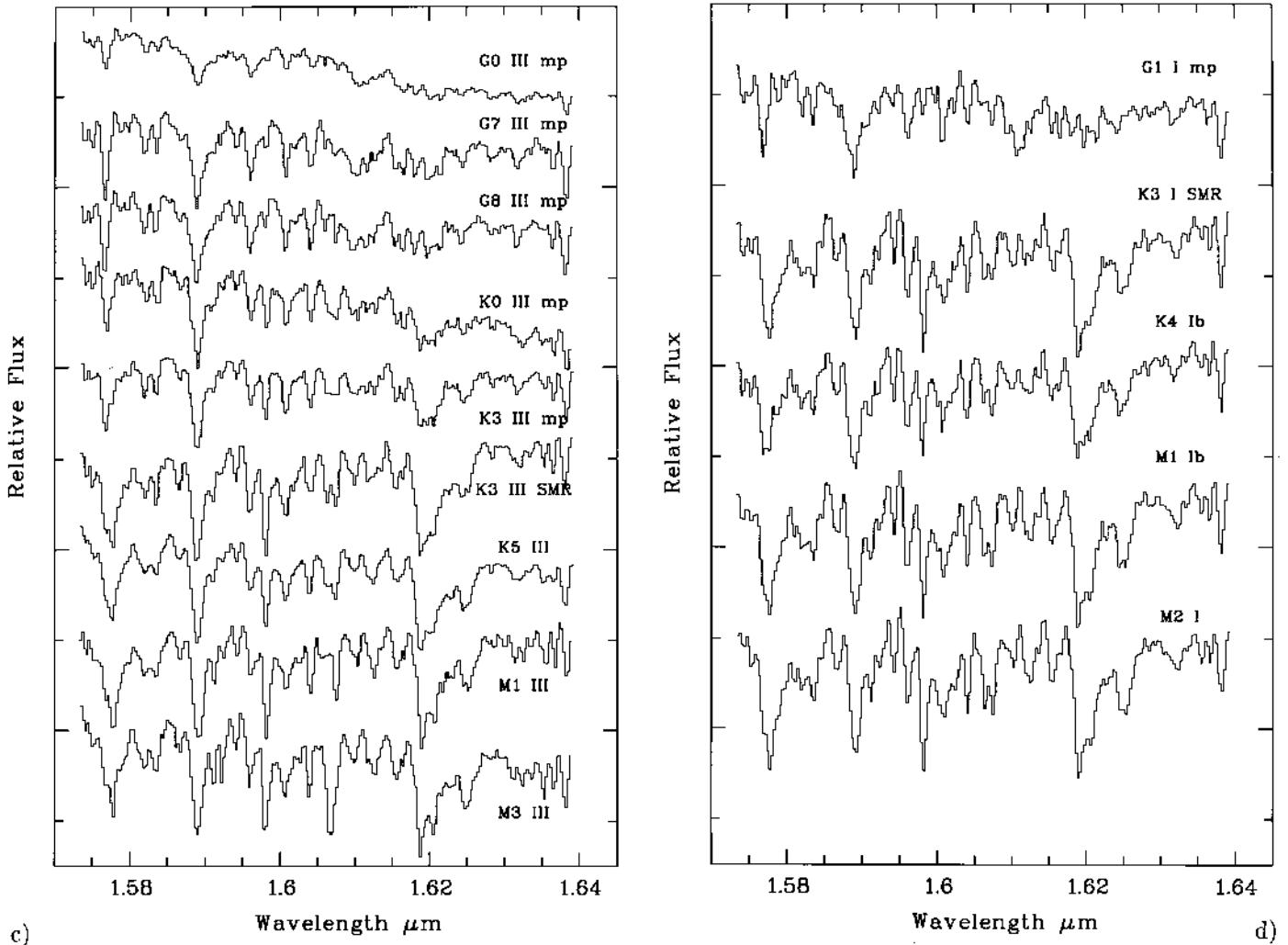
Fig. 2. continued

conditions were poor), second order correction was made by extracting a sky 1D spectrum from part of the slit away from the star. We relied on the 'master curve' for wavelength to grating position conversion provided at the beginning of the run. This was verified at beginning and middle of the run to always reproduce within half a pixel. One-dimension spectra have been extracted summing all relevant cross-sections on the two-dimension spectra.

For ISIS data, a combination of IRAF routines and ESO-MIDAS ones was used. Here also each frame was dark subtracted and flat-fielded using an external halogen lamp. Flats were also used to locate individual fibres on the chip ($x - y$ position and projected width). For each frame, a 1D spectrum from each fibre is then extracted. Spectra were wavelength calibrated using OH sky lines (see Oliva & Origlia 1992 for a table). The achieved precision is better than 1/7 pixel. Sky subtraction was then performed using the so-called 'sky fibres' as no dedicated

background exposures were taken. The main problem was that each fibre gives a slightly different spectral resolution, enough to produce P-Cygni profiles. We thus had to degrade all individual spectra (sky and object fibres) to the lowest resolution. Final stellar spectra were obtained by summing fibre 1D spectra with signal.

Relative flux calibration was performed using stars obtained during the same night as the objects of interest. During both runs primary flux standards from the lists in Koornneef (1983) and Bouchet et al. (1991) were observed. However, apart from BS4638, they are cool strong lined stars. So, hot stars with good published photometry (Gezari et al. 1993) were used as secondary standards. An asterisk in Table 1 marks all stars finally used as 'standards'. Black body were fitted to the published broad band magnitudes. It was verified that computed black body temperatures are in reasonable agreement with those expected from the star spectral type. Resulting

normalized flux calibration curves compare to a 3% level for the NTT data and to a 7% level for the ISIS one. Thanks to the relative flatness of cool star energy distribution in the small wavelength range considered, it appeared that all primary standards were suitable for relative flux calibration in spite of strong molecular band absorptions. Night averaged curves were used to calibrate both samples in relative flux. For a given star, the individual rectified spectra in the 3 wavelength ranges of IRSPEC data have different energy levels due to the use of an averaged calibration curve and to variable sky conditions. However in the overlapping segments, the spectral shapes agree very well, the individual spectra thus smoothly merged. Fluxes of the final spectra have been normalized to 1 in the range $1.59290-1.59506$ μm. A cross check of the quality of the relative flux calibration can be made by comparing stars observed with both spectrographs (see below).

Special care has been taken to correct from the atmospheric absorption features. BS 2456 (O7) and BS 6187 (O5) were frequently observed for that purpose at CFH and ESO respectively. These stars are featureless at the given resolution and in the considered wavelength range.

The wavelength range covers by the two sets of observations are very similar: it is 1.573 μm $-$ 1.646 μm at NTT and 1.578 μm $-$ 1.642 μm at CFHT. The main features in this range are the CO overtones (Δv=3) at 1.578, 1.598, 1.619 and 1.640 μm, and the OH absorption bands at 1.576, 1.604, 1.625 and 1.645 μm. A great number of metallic lines are also present in our stellar spectra. Among them is the strong SiI line at 1.589 μm. A detailed identification of all the lines has been done using the solar spectrum published by Livingston & Wallace (1991). Table 2 gives the line identifications with their wavelength. The wavelength range of integration used to measure the equivalent width (EW) is also given (last column).

4. Results

Representative spectra of stars from O to M for luminosity classes I, III and V are shown in Figs. 1 and 2 for the IRSPEC and ISIS sample respectively. Spectra are plotted in relative fluxes f_λ normalized to 1 in the range $1.59290-1.59506$ μm. Evolution of the depth of the absorption lines with spectral type is immediately apparent.

Figure 3 shows the spectra of HD 93800 obtained with both spectrographs. The similarity is remarkable. Note that the better spectral resolution of ISIS/IR allows to separate the numerous weak metallic lines present in cool stars. The difference in resolution explains the different depth (and width) of the lines. It will have consequences on the equivalent width values (see below).

In Table 3 are given the equivalent widths (in Å) of all the features for the whole sample of stars. A global continuum has been applied for each star, which accounts for the general shape of the spectrum. Features are labelled with
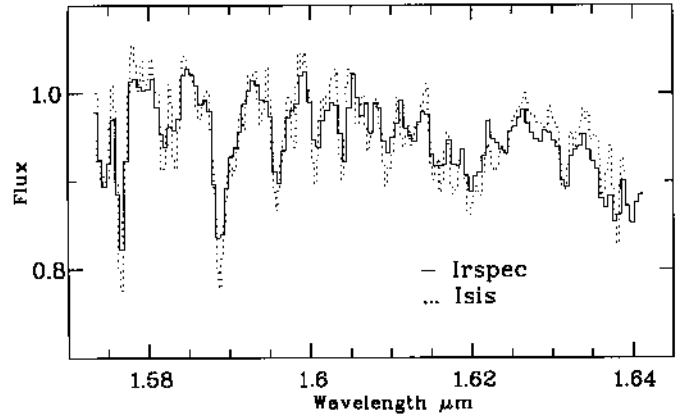
Fig. 3. Spectra of HD 93800 obtained with the IRSPEC and ISIS spectrographs. The difference in resolution explains the different depth of the lines. The better spectral resolution of ISIS/IR allows to separate the numerous weak metallic lines present in cool stars

the identification of the main line responsible for them. In fact, the feature labelled CO $\lambda1.58$ μ should be called MgI $\lambda1.577$ μ for dwarf stars as it is the dominant line (see Figs. 1 and 2). The wavelength range of integration is also given for the few hot stars as they are different from that of the cool stars (Table 2). Whenever stellar spectra of stars of the same spectral type are similar, they have been averaged. It is the case of two stellar spectra, BS5824 and BS6973 (K3III) in the IRSPEC sample, and of two others, BS2731 and HD 109655 (K5III) in the ISIS one. The listed equivalent widths are those of the averaged spectrum.

Comparing individual stars of same spectral type and/or stars observed more than once in the same configuration, the larger discrepancies are ΔEW=0.1 and ΔEW=0.3 Å for the strong and weak lines respectively. These are 'measurement' errors but the main source of uncertainty is really the assessment of the continuum level and shape. What appeared to be reasonable minimum and maximum levels of the continuum lead to at most 20% uncertainty on the measured EW.

The decrease of resolution between ISIS and IRSPEC precludes direct comparison. Indeed the effect of broadening due to lower resolution, is to decrease the measured equivalent widths. That the discrepancy between the two measurements (cf. Table 3) of the five stars in common in the IRSPEC and ISIS/IR samples (HD 93800, GL382, BS5020, BS4695, BS4902) is due to that problem was checked by degrading the ISIS/IR spectral resolution and remeasuring. Broadening correction curves at various spectral resolutions can in principal be constructed by measuring the EW after convolution of the initial spectrum with gaussians of different widths. However, this works only for isolated lines, the factor varying for line blends depending on the number and strength of the
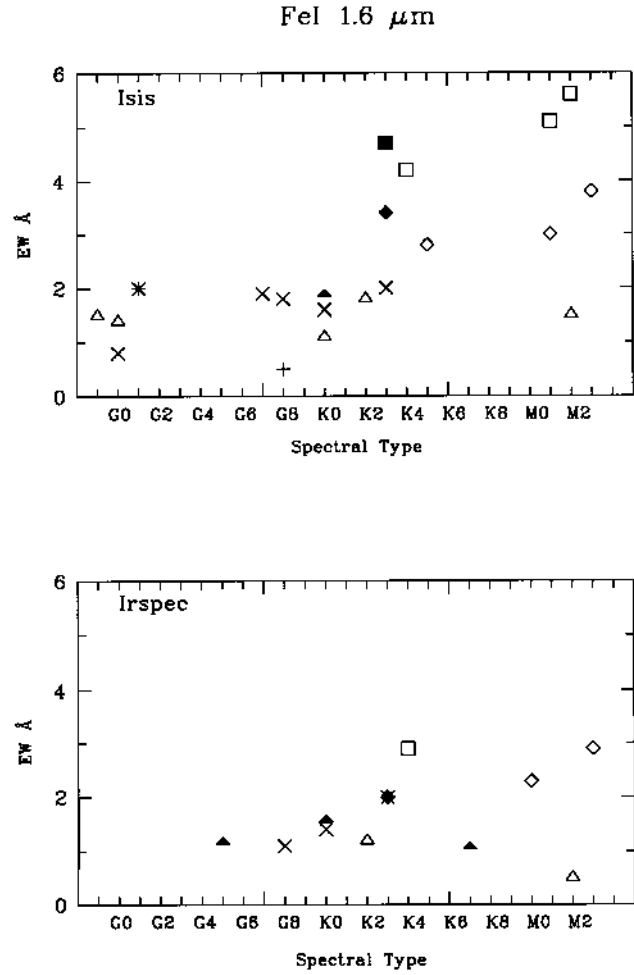
Table 3. Equivalent widths in Å

ISIS/IR DATA

	Br14+HeI 1.5855-1.5915	HeI 1.6062-1.6090	Br13 1.6090-1.6140
BS2456 O7	0.6		0.8
BS1879 O8	1.6	0.2	1.4
BS1123 B0V	1.7	0.4	1.8
BS5056 B1V	1.7	1.0	2.4
BS4590 B1.5V	2.1	0.8	1.7
BS4456 B4V	3.0		3.7
BS1790 B2III	2.6	0.7	2.4
BS4133 B1Ib	1.7	0.7	2.4

	CO 1.58	SiI +FeI	FeI 1.58	SiI 1.59	FeI 1.591	FeI 1.592	SiI 1.60	CO 1.60	FeI 1.60	OH 1.60	SiI +FeI	SiI +FeI	FeI +CaI	CO 1.62	CaI 1.62	FeI +OH	FeI +1.629	FeI 1.63	NiI +SiI
BS788 F9V	2.2	1.6	0.7	3.1	0.7	0.7	2.3	0.5	1.5	0.7	1.0	3.6	1.6	1.8	1.5	1.6	0.8	0.9	1.1
BS4983 G0V	1.8	1.3	0.6	2.8	0.6	0.6	1.9	0.4	1.4	0.9	0.9	3.0	1.4	1.5	1.5	1.1	0.8	1.3	1.4
BS4550 G8V mp	1.6	0.5	0.2	1.6	0.3	0.4	1.2	0.4	0.5	0.6	0.4	1.5	0.6	0.7	0.8	0.4	0.4	0.8:	0.1:
HD112758 K0V	2.7	1.3	0.7	3.3	0.7	0.5	2.1	0.6	1.1	0.6	1.1	2.2	1.4	1.8	1.8	1.4	0.4	1.1	1.4
HD93800 K0V SMR	3.4	2.6	0.8	4.4	1.3	0.9	3.1	0.9	1.9	1.2	1.5	3.7	2.1	2.7	2.6	1.9	0.4	1.5	2.5
HD115404 K2V	3.3	2.2	0.9	4.0	0.9	0.9	3.0	1.0	1.8	1.1	1.6	3.1	1.9	2.4	2.1	1.6	0.3	1.1	1.6
Gl382 M2V	3.0	1.6	0.6	2.5	0.6	0.9	1.8	0.8	1.5	1.6	1.5	2.8	2.3	2.1	2.3	2.3	0.7	1.7	1.8
BS4883 G0III mp	1.3	1.1	0.6	2.2	0.6	0.6	1.7	0.5	0.8	0.6	0.5	2.0	0.9	1.1	1.2	1.1	0.7	1.0	0.7
BS3903 G7III mp	2.6	1.7	0.7	3.6	0.9	0.7	2.4	0.7	1.9	1.2	1.3	4.3	1.9	2.2	2.1	1.9	1.2	1.8	1.9
BS5020 G8III mp	2.8	2.1	0.7	3.7	0.8	0.6	2.1	0.5	1.8	1.1	1.3	3.8	1.6	2.0	1.7	1.5	0.8	1.3	1.7
BS4695 K0III mp	2.7	1.9	0.4	3.5	0.9	0.5	1.4	1.2	1.6	0.8	1.4	2.4	1.5	2.3	2.0	2.0	0.8	2.1	2.2
BS5315 K3III mp	3.4	1.9	0.5	3.5	0.8	0.4	1.7	1.4	2.0	1.2	1.6	2.7	1.4	2.7	2.2	2.1	0.7	1.2	1.8
HD111180 K3III SMR	6.3	3.6	1.1	4.6	1.2	0.9	2.6	3.0	3.4	1.6	2.4	2.9	1.6	4.4	3.4	3.4	0.3	1.0	1.3
HD109655 BS2731, K5III	4.6	2.4	0.6	4.1	1.0	0.9	2.2	2.7	2.8	1.6	2.1	2.2	1.1	3.8	3.3	3.4	0.5	1.1	1.6
BS4127 M1III	5.8	3.2	0.6	4.2	1.0	0.9	1.8	2.8	3.0	1.8	2.2	2.6	1.3	3.8	3.8	4.0	0.8	1.8	1.8
BS4902 M3III	5.5	3.6	0.9	4.7	1.4	1.4	2.6	3.4	3.8	2.2	3.9	2.9	1.7	4.3	3.8	4.3	0.8	2.5	2.6
BS3459 G1I mp	2.7	2.1	1.1	4.5	1.1	1.0	2.4	0.8	2.0	0.9	1.4	5.2	1.9	2.2	2.1	2.5	1.2	1.5	1.7
BS2764 K3I SMR	7.4	4.5	1.0	4.9	1.4	1.1	2.7	3.8	4.7	2.1	2.8	4.1	2.0	5.0	4.5	5.1	1.8	2.7	2.4
BS1112 K4Ib	7.2	4.6	1.3	5.3	1.5	1.4	3.4	3.0	4.2	2.1	2.8	4.3	2.3	4.5	3.7	4.3	1.4	1.9	2.1
BS3170 M1Ib	8.5	5.6	1.4	5.5	1.7	1.7	3.3	3.9	5.1	2.5	3.5	4.4	2.4	5.1	4.5	5.3	1.3	2.6	2.3
BS3364 M2I	9.4	5.8	1.3	5.6	1.6	1.7	2.8	4.2	5.6	2.8	3.9	4.3	2.2	5.3	5.0	5.8	1.5	2.8	2.5

IRSPEC DATA

	CO 1.58	SiI +FeI	FeI 1.58	SiI 1.59	FeI 1.591	FeI 1.592	SiI 1.60	CO 1.60	FeI 1.60	OH 1.60	SiI +FeI	SiI +FeI	FeI +CaI	CO 1.62	CaI 1.62	FeI +OH	FeI +1.629	FeI 1.63	NiI +SiI
HD160691 G5V SMR							2.4	0.6	1.2	1.0	0.6	2.2	1.3	1.4	1.2	0.5	0.2	1.1	2.0
HD93800 K0V SMR	3.5	2.3	0.4	3.7	1.1	0.8	2.5	0.9	1.6	1.4	1.0	2.7	1.6	1.9	1.9	1.1	0.4	1.4	2.2
HD130871 K2V	3.2	2.1	0.4	3.3	0.8	0.6	2.0	0.6	1.2	1.1	0.7	2.0	1.4	1.5	1.3	0.8	0.3	1.4	2.1
HD157881 K7V SMR	4.0	2.1	0.4	3.5	0.9	0.6	2.0	0.7	1.1	1.3	0.8	1.8	2.1	2.1	1.8	1.1	0.2	1.5	2.3
Gl382 M2V	2.1	0.7	0.1	1.6	0.4	0.4	0.7	0.4	0.5	0.9	1.0	1.2	1.9	1.4	1.6	1.2	0.3	0.9	1.2
BS5020 G8III	1.1	1.1	0.2	2.8	0.7	0.4	1.6	0.6	1.1	0.9	0.6	2.6	1.2	1.6	1.4	0.8	0.3	1.1	2.1
BS4695 K0III mp	2.1	1.3	0.3	3.0	0.7	0.3	1.0	0.9	1.4	0.9	0.6	1.6	0.8	1.8	1.3	1.1	0.3	0.9	1.6
BS5824 BS6973, K3III mp	3.1	2.0	0.4	3.5	1.0	0.7	2.1	1.5	2.0	1.5	0.7	2.3	1.4	2.7	2.0	1.6	0.5	1.1	1.9
HD175674 K3III SMR	3.9	3.0	0.5	3.5	1.0	0.8	1.9	1.5	2.0	0.9	1.0	1.8	1.1	2.6	1.1				
BS4174 M0III	4.5	2.5	0.3	3.2	0.9	0.5	1.2	1.9	2.3	1.6	1.8	1.7	1.0	2.7	2.9	2.6	0.4	1.1	1.9
BS4902 M3III	5.0	2.9	0.4	3.6	0.9	0.8	1.4	2.6	2.9	1.3	2.0	1.4	1.6	4.0	4.0	3.6	0.1	1.2	1.6
BS5645 K4I	5.7	3.8	0.5	3.8	1.0	0.7	1.6	2.6	2.9	1.7	1.7	1.6	1.2	3.9	3.0	2.7	0.4	1.2	2.0

OH 1.6 μm

FeI 1.6 μm
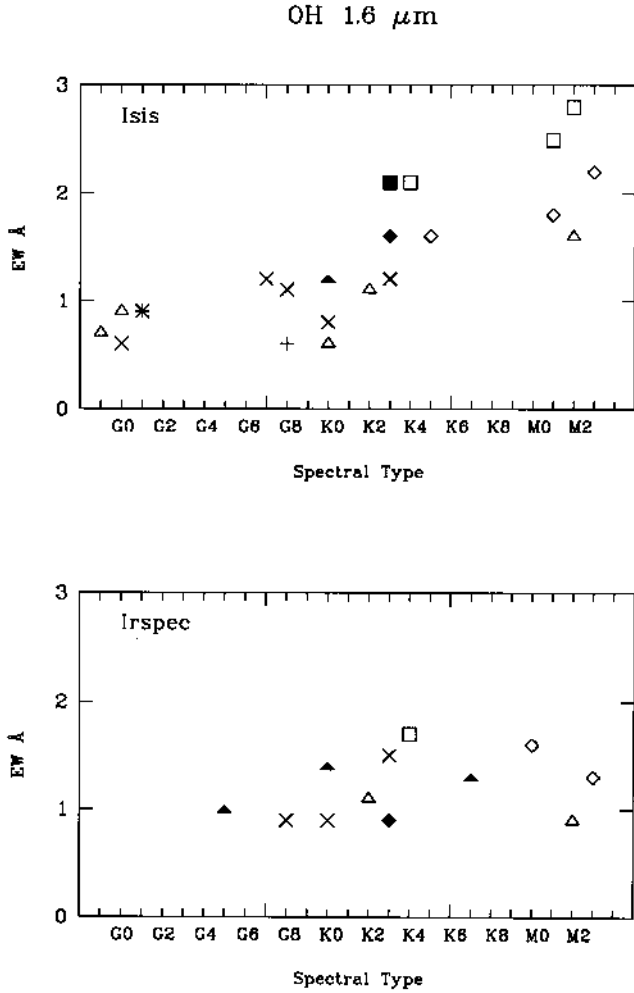
Fig. 4. Variations of OH 1.60 μm with spectral type and luminosity class. Open symbols are for normal abundance stars, filled symbols are for SMR stars and crosses for underabundant ones. □, ■ and ∗: supergiants; ◇, ◆ and ×: giants; △, ▲ and +: dwarfs

Fig. 5. Variations of FeI 1.60 μm with spectral type and luminosity class. Same symbols as in Fig. 4

included lines. To create a stellar library merging both samples, ISIS spectra have to be degraded to the resolution of the IRSPEC ones. However, for stellar population synthesis of a galaxy observed with the best resolution, only the limited - better resolved - library will be available, except if the galactic velocity dispersion is high. In that case the whole stellar library has in fact to be degraded to the dispersion of the galaxy.

Two stars of our sample (BS5645 and BS3364) are found in Origlia et al. (1993). These authors give the equivalent width of two strong features, SiI 1.59 μm and CO 1.62 μm. However they used a local continuum and wider integration bands. To compare with their results, EW of both lines were remeasured following the prescription as given in their Sect. 2.2. For BS3364, we also had to degrade the resolution to match IRSPEC. For BS5645,

our new EW are 0.3 Å lower for both lines. In the case of BS3364, they are 0.4 Å larger. This is within the above quoted errors when one also keeps in mind that we had to degrade ISIS resolution. A priori, for stellar population synthesis at a resolution lower or equal to 1500, their library can be added to the one presented here.

In Figs. 4 to 6 are given the variation of, respectively, OH 1.60 μ, FeI 1.60 μm and CO 1.62 μm as a function of spectral type and luminosity class, for both sets of data. Normal stars are plotted together with over and under abundant stars, printed with different symbols. In spite of the small number of stars, general tendencies can be inferred. The discussion below applies to both samples although they are presented separately because of the small shift in EW due to the difference in resolution as explained above.

First, all three lines are good indicators of the effective temperature, being stronger in cooler stars. Note how close are the behaviour of the CO and Fe features.

CO 1.62 μm

CO 1.62 / SiI 1.59
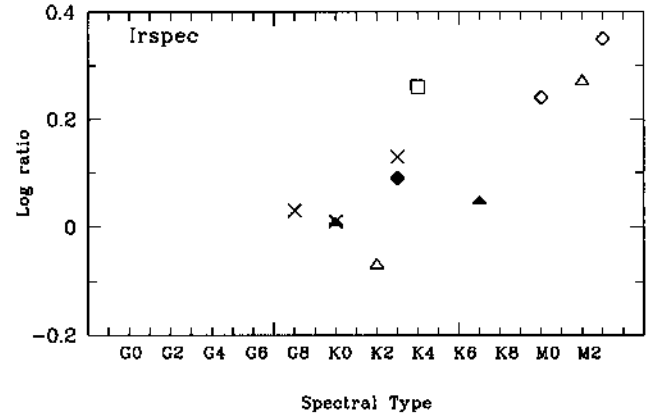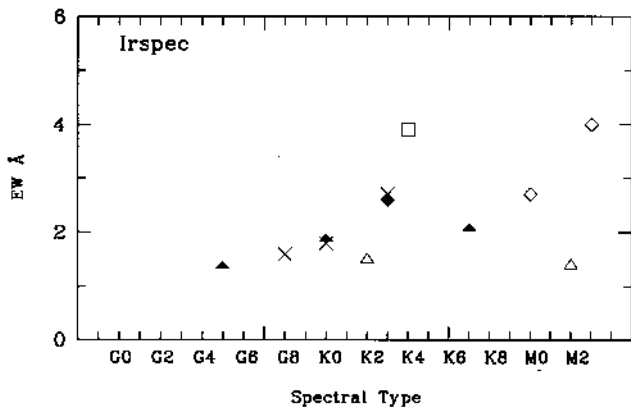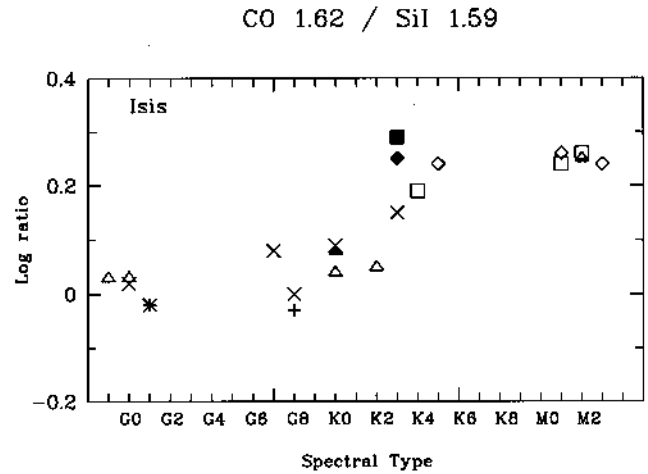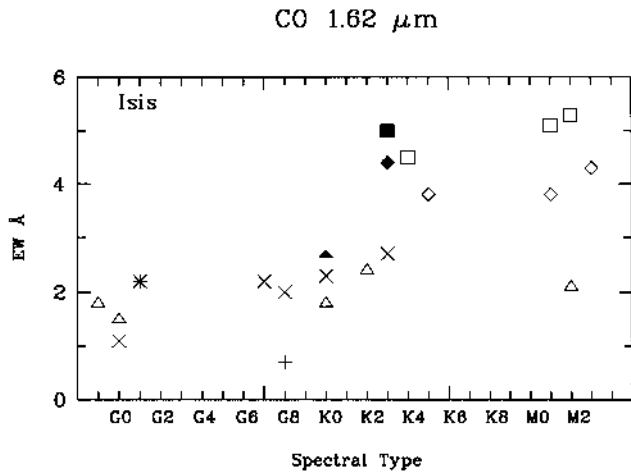
Fig. 6. Variations of CO 1.62 μm with spectral type and luminosity class. Same symbols as in Fig. 4

Fig. 7. Variations of the line ratio, (CO+CaI) 1.62 μm over SiI 1.59 μm, with spectral type and luminosity class. Same symbols as in Fig. 4

Second, although none of these lines are strong luminosity class indicators, CO and FeI discriminate pretty well supergiants from dwarfs and giants. Their equivalent widths are clearly larger than those of the less luminous stars.

Third, it has to be emphasised that stars plotted as normal-abundance stars are actually stars for which abundances are not known. Some of them could have in fact non solar abundances. It could be the case for the dwarf GL 382 (M2V) the lines of which are systematically weaker than expected for a M2 star if it follows the general trend of the more luminous stars. GL 382 could then be an underabundant star. However a similar trend appears in the K and M dwarf stellar spectra in Lançon & Rocca-Volmerange (1993) where IR stellar features are maximum in K3V type and decrease beyond.

We also plot, Fig. 7, the variation of the line ratio (CO+CaI)λ1.62/SiIλ1.59 as a function of spectral type as it extends to stars warmer than the one presented by

Origlia et al. (1993). CO+CaI had to be plotted to be comparable to their broad feature. This ratio is actually a very good temperature indicator but it does not allow any discrimination between luminosity classes or metallicity ranges as a consequence of the sensitivity of both lines on luminosity and metallicity. For IRSPEC data, the slope and scatter of the relation is the same as the one obtained by Origlia et al. For the ISIS data, although the scatter is of the same order, the relation is along a different slope due to the presence, here, of G stars.

In Fig. 8 is plotted COλ1.60/SiIλ1.60, a very good luminosity discriminator for stars later than K0. This is indeed obvious by inspection of Figs. 1 and 2. The advantage of this ratio is that both lines are next to each other so that they can be observed at the same time and do not suffer from any reddening problem.

CO 1.6 / SiI 1.6
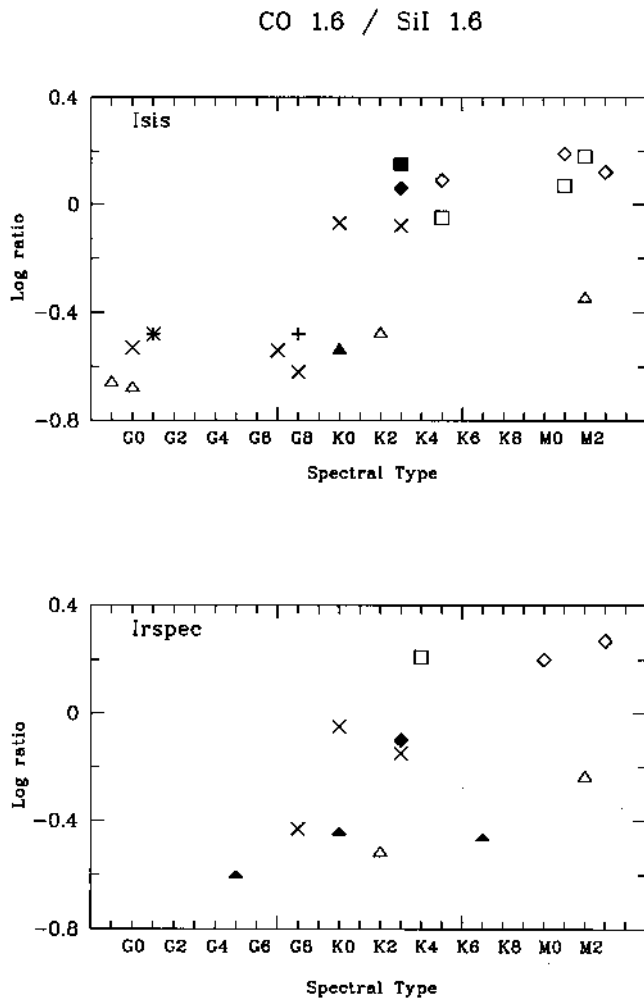
Fig. 8. Variations of the line ratio, CO 1.6 μm over SiI 1.6 μm, with spectral type and luminosity class. Same symbols as in Fig. 4

The spectra, at their full spectral resolution, are accessible in electronic form through the Centre de Données Stellaire in Strasbourg.

References

Arnaud K.A., Gilmore G., Collier Cameron A., 1989, MNRAS 237, 495

Barbuy B., Grenon M., 1990, ESO Conf. Proc. 35 "Bulge of galaxies". In: Jarvis B.J. and Terndrup D.M. (eds.), La Serena

Bell R.A., Briley M.M., Smith G.H., 1990, AJ 100, 187

Bouchet P., Manfroid J., Schmider F.-X., 1991, A&AS 91, 409

Casali M.M., Matthews H.E., 1992, MNRAS 258, 399

Cayrel de Strobel G., 1991, conf. proc. "evolutionary phenomena in the Universe", p. 27

Cayrel de Strobel G., Hauck B., François P., et al., 1992, A&AS 95, 273

Dallier R., 1995, PhD Thesis, Paris 7 University

Davidge T.J., 1990, AJ 99, 561

Davidge T.J., 1992, AJ 103, 1512

Davidge T.J., Boeshaar P.C., 1993, ApJ Lett. 403, L47

Delisle S., Hardy E., 1992, AJ 103, 711

Gaffney N.I., Lester D.F., 1992, ApJ 394, 139

Gezari D.Y., Schmitz M., Pitts P.S., Mead J.M., 1993, Nasa Ref. Pub. 1294, " Catalog of IR observations", 3rd edition

Gredel R., Moorwood A.F.M., 1991, IRSPEC-ESO operating manual

Kleinmann S.G., Hall D.N.B., 1986, ApJS 62, 501

Koorneef J., 1983, A&AS 51, 489

Lançon A., Rocca-Volmerange B., 1992 A&AS 96, 593

Livingston W., Wallace L., 1991, N.S.O. Technical report 91-001, National Solar Observatory, Tucson

McWilliam A., 1990, ApJS 74, 1075

Mould J.R., 1978, ApJ 226, 923

Oliva E., Origlia L., 1992, A&A 254, 466

Origlia L., Moorwood A.F.M., Oliva E., 1993, A&A 280, 536

Simons D., 1993, The RedEye Camera, 'CFHT user's manual'

Taylor B.J., 1991, ApJS 76, 715

Terndrup D.M., Frogel J.A., Whitford A.E., 1991, ApJ 378, 742

Tsuji T., 1986, A&A 156, 8

Tsuji T., 1991, A&A 245, 203

Vila-Costas M.B., Edmunds M.G., 1992, MNRAS 259, 121

Zhou X., 1991, A&A 248, 367